Journal of Chromatography A, 1235 (2012) 39–48

Contents lists available at SciVerse ScienceDirect

Journal of Chromatography A

journal homepage: www.elsevier.com/locate/chroma

Pareto-optimality study into the comparison of the separation potential of comprehensive two-dimensional liquid chromatography in the column and spatial modes

Dominique J.D. Vanhoutte, Gabriel Vivó-Truyols*, Peter J. Schoenmakers

Analytical-Chemistry Group, Van't Hoff Institute for Molecular Sciences, University of Amsterdam, P.O. Box 94157, 1090 GD Amsterdam, The Netherlands

ARTICLE INFO

Article history:
Received 18 October 2011
Received in revised form 12 January 2012
Accepted 20 January 2012
Available online 25 January 2012

Keywords:
Two-dimensional liquid chromatography
LC × LC
Spatial chromatography
OPTLC

ABSTRACT

The expected performance of spatial ("flat-bed") two-dimensional liquid chromatography (^{x}LC × ^{x}LC) has been calculated using the Pareto-optimality strategy. This approach allowed different objectives (total peak capacity, total analysis time, and total dilution) to be considered simultaneously and to establish optimal parameters (pressure drop, particle size, bed length, and initial spot size). The performance of spatial two-dimensional chromatographic systems was compared with that of conventional on-line, real-time two-dimensional column-liquid-chromatography systems (^{t}LC × ^{t}LC). The potential gain in peak capacity and/or analysis time of the spatial configuration was confirmed. By restricting the spatial parameters to realistic chromatographic conditions (limiting the stress, as counterbalance for the pressure drop through the sorbent bed, to 2500 kg) it was found that ^{x}LC × ^{x}LC is attractive for very fast analysis of complex samples, rather than for extremely efficient separations. For example, a peak capacity of 780 may be achieved in only 2.7 min using a 100 × 100 mm sorbent bed of a quality currently encountered thin-layer chromatography. Furthermore, if beds can be packed as efficiently as contemporary columns, the predicted peak capacity increases to around 1000, corresponding to a peak-production rate of about 6.3 peaks/s. Possibilities to boost the performance of ^{x}LC × ^{x}LC further are briefly discussed. Unless we can overcome the severe stress requirements of high-performance ^{x}LC × ^{x}LC, conventional ^{t}LC × ^{t}LC may be more amenable to very complex separations, thanks to the very high peak capacities. However, ^{t}LC × ^{t}LC separations will require long analysis times (*e.g.* 10,000 peaks in 37 h, corresponding to 0.075 peaks/s at a pressure drop of 40 MPa). The best trade-off between total peak capacity, total analysis time, and total dilution under restricted (realistic) conditions was obtained using high pressures, small chromatographic beds, small particles, and relatively large sample spots.

1. Introduction

Modern liquid chromatography is all about resolving the highest number of peaks in the shortest possible time. To realize this, high system performances are indispensable. A way to express the separation potential of a chromatographic system is the peak capacity, n_c. This parameter was introduced by Giddings in 1967 as a measure for the number of peaks that can be located – at equal resolution – between the first (unretained) and the last (most retained) peaks in a chromatogram [1]. However, a statistical treatment, assuming the peaks to be distributed randomly, has revealed that the number of single-component peaks cannot exceed about 18% of the peak capacity [2]. Furthermore, the expected total number of peaks p (*i.e.* singlets, doublets, triplets, *etc.*) can be expressed by [2]:

$$p = me^{-m/n_c} \quad (1)$$

where m is the number of components in the sample and n_c the peak capacity.

In the field of systems biology (proteomics, metabolomics, *etc.*) very complex samples are frequently encountered. A typical proteome sample may contain 10,000–50,000 different proteins or – in case these proteins are digested prior to analysis – 100,000–500,000 different peptides [3]. It is clear from Eq. (1) that it is virtually impossible to separate all the components in such a complex sample. However, irrespective of the complexity of the sample, maximizing the number of separated components can only be achieved through maximizing the peak capacity of the chromatographic system (Eq. (1)).

The most straightforward approach to increase the peak capacity in one-dimensional liquid chromatography (1D-LC) is to

* Corresponding author. Tel.: +31 20 525 6531; fax: +31 20 525 5604.
E-mail address: g.vivotruyols@uva.nl (G. Vivó-Truyols).

0021-9673/$ – see front matter © 2012 Elsevier B.V. All rights reserved.
doi:10.1016/j.chroma.2012.01.059

increase the number of plates, *N*. Many theoretical and experimental studies into achieving high peak capacities in one-dimensional column LC (1D-^{t}LC) have been published [4–15]. For example, Shen et al. realized a peak capacity of 1500 for the separation of a tryptic digest of *Shewanella oneidensis* in approximately 33 h with gradient-elution reversed-phase LC (RPLC), using a 2 m × 50 μm I.D. fused-silica column packed with 3.0-μm porous C_{18} particles [14]. Eeltink et al. recently obtained a peak capacity exceeding 1000 in 10 h for the separation of a proteolytic digest of *Escherichia coli* in RPLC, using a monolithic poly(styrene-*co*-divinylbenzene) capillary column of 1 m length [4]. The law of diminishing returns is, however, merciless in 1D-LC. Once n_c is large, even a slight increase will require a very much longer analysis time [16]. For separating the proteomics samples mentioned above 1D-LC clearly falls way short.

Potentially, a much more favourable trade-off can be achieved in comprehensive two-dimensional column LC (commonly LC × LC, but in the context of the present paper denoted as ^{t}LC × ^{t}LC). In this configuration, the theoretical total peak capacity of the two-dimensional set-up $^{2D}n_c$ equals the product of the peak capacities obtained in each dimension separately, whereas the total analysis time $^{2D}t_w$ equals the sum of the analysis times for each dimension [17,18]. The first-dimension separation is usually very slow, but the peak capacity can be increased by an order of magnitude in comparison with 1D-LC, while keeping the analysis time within reasonable limits. However, to make full use of this gain in peak capacity, ^{t}LC × ^{t}LC should make use of two completely different (independent or "orthogonal") separation mechanisms. Any correlation between the retention times in the two dimensions will result in a decrease in the effective peak capacity and the experimentally obtained n_c values will be lower than the product of the peak capacities in the individual dimensions.

Two-dimensional (liquid) chromatographic separations can be divided into two categories, *i.e.* time-based (^{t}LC × ^{t}LC) and spatial (^{x}LC × ^{x}LC) separations. Time-based LC (^{t}LC) is associated with the traditional "column" chromatography, in which solutes are eluted from the separation body to be detected. In the case of spatial chromatography (^{x}LC) the solutes migrate to specific positions in the separation body. In ^{t}LC × ^{t}LC small consecutive fractions from the first dimension are injected in the second dimension. The resulting series of second-dimension chromatograms can be visualized as a two-dimensional color map. In spatial two-dimensional chromatography, the separation is carried out physically in a two-dimensional flat bed, separating the compounds in one direction (first dimension) and then in a perpendicular direction (second-dimension). The compounds may be detected in the two-dimensional plane (^{x}LC × ^{x}LC) or they may be eluted from the bed during the second-dimension separation (^{x}LC × ^{t}LC).

Comprehensive two-dimensional column LC can be operated in either an on-line (^{t}LC × ^{t}LC) or off-line (^{t}LC/×/^{t}LC) mode. In the on-line mode, the second-dimension separations are carried out during the first-dimension elution. In order for a first-dimension peak to be sampled in several second-dimension runs the first dimension should be (very) slow and the second one (very) fast. In the off-line mode, a fraction collector is used to store fractions from the first dimension, carrying out the second-dimension runs in an independent second step. Stop-flow on-line ^{t}LC × ^{t}LC [19] is a compromise in which the times are decoupled, but the sample remains confined within a single instrument. Both on-line and off-line modes have advantages and disadvantages. When the total analysis time is an issue, on-line ^{t}LC × ^{t}LC is usually preferred. However, this approach has a limited separation power due to the short analysis time available in the second dimension. In ^{t}LC × ^{t}LC the second-dimension separation can be viewed as a detector of the first-dimension separation. In order to preserve the separation obtained in the first dimension the eluting peaks should be sampled with sufficient frequency. However, this is not possible because of time limitations. In practice, one accepts a certain decrease in the actual first-dimension peak capacity due to "undersampling" first-dimension peaks and the resulting additional band broadening in the first dimension [20–22]. Furthermore, the second-dimension chromatogram is likely to suffer from injection band broadening, since relatively large volumes of effluent from the first-dimension separation are injected on the second-dimension column. This effect has a negative impact on the second-dimension peak capacity. In the end, the modulation time should be carefully optimized, taking into account all these effects to reach the best possible compromise [23].

Most separations described in literature using the on-line configuration required analysis times of less than 2 h and produced peak capacities between 500 and 1000 [24]. For example, Stoll et al. claimed a peak capacity of 1024 for an on-line ^{t}LC × ^{t}LC separation of plant metabolites in roughly 30 min, corresponding to a peak-production rate of more than 0.5 peaks/s [24,25].

When a high peak capacity is the main objective and the total analysis time is not constrained, off-line ^{t}LC/×/^{t}LC may be preferred. Very long analysis times may be required. For example, Eeltink et al. obtained a peak capacity of 8720 for an off-line 2D-LC separation of an *E. coli* digest in 1560 min, which corresponds to a peak-production rate of about 0.1 peaks/s [26].

A potential way to overcome the limitations of comprehensive two-dimensional column LC is two-dimensional spatial chromatography (^{x}LC × ^{x}LC). Analytes are separated in a porous flat bed to end up at specific locations in the separation medium, rather than specific elution times. Typically, a sample may be injected at (or close to) a corner of the plane and then eluted along the *x*-axis by pumping an appropriate solvent in the direction parallel to that axis. After a certain time the flow of the first dimension solvent is stopped and a second solvent is pumped in the perpendicular direction (along the *y*-axis of the plane) resulting in migration of the analytes in the second dimension. This implies that each separated compound of the sample may ultimately be characterized by a combination of its *x* and *y* coordinates. As before, a high degree of orthogonality between the two separation dimensions is required to make full use of the total two-dimensional peak capacity. This may, for example, be achieved by packing a narrow strip at the edge of the (*x* direction) with a material that is different from that used in the rest of the plane [27,28], by using strongly different mobile-phase conditions for each dimension [28], or by combining electrically driven and pressure-driven separations [29]. No fraction collection or valve switching is required for ^{x}LC × ^{x}LC, but the overriding argument in its favour is that all second-dimension separations are performed simultaneously. This fundamentally implies that shorter analysis times and higher peak capacities can be achieved in comparison with column-based ^{t}LC × ^{t}LC.

Prime examples of spatial two-dimensional separations are two-dimensional polyacrylamide gel electrophoresis (2D-PAGE) and two-dimensional thin-layer chromatography (2D-TLC). The former technique is known to have a very high resolving power (peak capacities up to 10,000 have been demonstrated [30]), but it has some important drawbacks. 2D-PAGE is labor-intensive and difficult to automate. It has a limited loading capacity and low efficiency in the analysis of hydrophobic proteins, it is time-consuming, and it cannot be coupled on-line with mass-spectrometric (MS) detection [31–33].

To increase the separation power of conventional TLC, forced-flow (thin) layer chromatographic techniques have been introduced already in the late 1970s. One of these techniques is over-pressured thin-layer chromatography (OPTLC) [34]. The key feature of this approach lies in the fact that the mobile phase does not flow due to capillary action under atmospheric conditions, but is driven by pressure. A closed-bed compartment and a pump are

used to push the mobile phase through the separation medium. This results in a constant mobile-phase velocity. The most modern commercially available OPTLC systems allow operating pressures up to 5 MPa (50 bar) and, consequently, small particles [35–37].

OPTLC devices are basically designed to perform one-dimensional separations, but researchers have tried to come up with similar instrumentation for two-dimensional separations. A generalization of the concept was already published in the 1980s by Guiochon et al. [27,38]. However, the practical implementations have been quite limited so far [29,39,40]. A theoretical study into the potentially attainable peak capacity in such a two-dimensional set-up was published by Guiochon et al. [18,28].

In the present study we have performed theoretical computations to compare the trade-off between time and peak capacity for ${}^{t}\mathrm{LC}\times{}^{t}\mathrm{LC}$ and ${}^{x}\mathrm{LC}\times{}^{x}\mathrm{LC}$. As a basis for this comparison we used the concept of Pareto optimization to establish optimal (system) conditions for both types of two-dimensional chromatography, in such a way that maximum peak capacities and minimum analysis times could be obtained. Pareto optimization has already been applied to ${}^{t}\mathrm{LC}\times{}^{t}\mathrm{LC}$, taking into account the effects of additional band broadening (undersampling in the first dimension and injection band broadening in the second dimension) and dilution of the sample in both dimensions for both isocratic and gradient-elution experiments [23]. However, to our knowledge, the concept has not yet been applied to ${}^{x}\mathrm{LC}\times{}^{x}\mathrm{LC}$. We were able to apply the Pareto-optimization concept to this type of chromatography by taking the theoretical equations developed by Guiochon et al. for peak capacity in ${}^{x}\mathrm{LC}\times{}^{x}\mathrm{LC}$ [18] as a starting point. We established new equations to account for dilution of the sample in each dimension. We focused on chromatographic conditions that are currently accessible (pressure limit 5 MPa and particle sizes down to 4 μm).

The goal of this study was not only to find optimal conditions for two-dimensional spatial chromatography, but also to estimate the gain in analysis time that ${}^{x}\mathrm{LC}\times{}^{x}\mathrm{LC}$ entails in comparison with ${}^{t}\mathrm{LC}\times{}^{t}\mathrm{LC}$ for specific peak capacities. This gain is calculated taking into account the total stress experienced by the chromatographic system, which in ${}^{x}\mathrm{LC}\times{}^{x}\mathrm{LC}$ is proportional to the pressure drop. By restricting this total stress to 2500 kg, a realistic estimate of the potential performance of ${}^{x}\mathrm{LC}\times{}^{x}\mathrm{LC}$ can be obtained. In addition, the system was investigated for a three-goal trade-off between (maximum) peak capacity, (minimum) analysis time and (minimum) dilution.

2. Theory

In this section, equations that link several chromatographic parameters necessary for the calculation of the total analysis time and the total peak capacity will be presented. Subsequently, these equations will be applied as part of the Pareto optimization of two-dimensional spatial chromatography and the results will be compared with those obtained for ${}^{t}\mathrm{LC}\times{}^{t}\mathrm{LC}$ [23].

2.1. General equations for ${}^{x}LC\times{}^{x}LC$ and ${}^{t}LC\times{}^{t}LC$

The pressure drop across a chromatographic system (ΔP) can be expressed by Darcy's equation:

$$\Delta P = \frac{u_m \phi \eta L}{d_p^2} = \frac{\phi \eta L^2}{t_m d_p^2} \tag{2}$$

in which u_m is the linear velocity corresponding to an unretained compound, ϕ is the flow-resistance factor, η the mobile-phase viscosity, L the length of the column (or the bed), and d_p the particle size. The right-hand side of Eq. (2) uses implicitly the definition of linear velocity, *i.e.* $u_m = L/t_m$, with t_m being the time required for an unretained compound to reach the end of the stationary phase. As was already discussed in [23], according to Cramers et al. [41] u_m should be defined as the velocity of the mobile phase corresponding to an unretained compound able to fully penetrate the stationary phase pores. This convention was therefore followed throughout this paper. The flow-resistance factor is affected by the choice of this convention. Appropriate values were used in the present study.

Concerning the pressure drop, it was assumed in this work that the chromatographic system is running continuously under the maximum allowable pressure defined by the manufacturer, *i.e.* 40 MPa and 5 MPa for time-based and space-based chromatographic instruments, respectively.

A general way to express the efficiency of a chromatographic system is to use the reduced van-Deemter equation:

$$h = a + \frac{b}{\nu} + c\nu \tag{3}$$

where h represents the reduced (dimensionless) plate height ($h = H/d_p$ with H being the plate height), and a, b, and c are coefficients related to the Eddy diffusion, molecular diffusion, and mass-transfer contribution, respectively. In Eq. (3) ν is the reduced velocity that can be expressed as

$$\nu = \frac{u_m d_p}{D_m} \tag{4}$$

in which D_m is the molecular diffusion coefficient of the analyte in the mobile phase.

For a two-dimensional chromatographic system, the theoretical total analysis time (${}^{2D}t_w$) and total peak capacity (${}^{2D}n_c$) can be calculated using the following equations [17,18]

$${}^{2D}t_w = {}^{1}t_w + {}^{2}t_w \tag{5}$$

$${}^{2D}n_c = {}^{1}n.{}^{2}n \tag{6}$$

where ${}^{1}t_w$ and ${}^{2}t_w$ are the analysis times in the first- and second-dimension, respectively, and ${}^{1}n$ and ${}^{2}n$ the peak capacities in these two dimensions. Eqs. (5) and (6) illustrate the advantage of two-dimensional chromatography with respect to one-dimensional chromatography in terms of speed and peak capacity. As peak capacities are multiplied, while retention times are summed, a much higher separation power can be obtained in an only slightly longer analysis time.

Commonly, the retention factor k is defined as

$$k = \frac{V_R - V_m}{V_m} \tag{7}$$

where V_R is the elution volume of a compound of interest and V_m the elution volume of an unretained compound.

2.2. Calculation of total peak capacity and analysis time in ${}^{x}LC\times{}^{x}LC$

Note that, in spatial chromatography, the retention factor is written as follows:

$$k = \frac{V_R - V_m}{V_m} = \frac{L - x_R}{x_R} \tag{8}$$

where x_R is the position of a compound along the chromatographic bed. It follows that

$$x_R = \frac{L}{k+1} \tag{9}$$

Guiochon et al. derived the theoretical equation for the two-dimensional peak capacity in spatial chromatography [18,28]. Introducing Eq. (4) and assuming a thin-layer packed with silica particles, which is subsequently developed in two directions and

assuming that the first dimension flow is stopped when a non-retained compound reaches the edge of the bed, one obtains

$$^{2}n_{spatial} = \frac{1}{4H^2}\left(\sqrt{\sigma_i^2 + LH\left(1+\frac{2\gamma}{h\nu}\right)} - \sqrt{\sigma_i^2 + \frac{2\gamma LH}{h\nu}}\right)^2 \quad (10)$$

in which σ_i is the standard deviation of the sample spot and γ the bed tortuosity. This equation is only valid in the case in which the bed and diffusion characteristics (H, D_m, L and u_m) are considered to be equal in both directions and the concentration profiles of the sample spot follow a Gaussian distribution in both directions [18,28]. These assumptions have been made throughout the present paper.

In the case in which the initial sample spot is negligibly small ($4\sigma_i \ll 4\sqrt{(2\gamma LH/h\nu)}$), the equation can be simplified to

$$^{2}n^{*}_{spatial} = \frac{L}{4H}\left(\sqrt{1+\frac{2\gamma}{h\nu}} - \sqrt{\frac{2\gamma}{h\nu}}\right)^2 \quad (11)$$

In spatial chromatography the mobile-phase flow is stopped in each dimension when an unretained compound reaches the edge of the bed. Therefore, the total development time in spatial chromatography can be expressed as

$$^{2D}t_{w,spatial} = {}^{1}t_w + {}^{2}t_w = {}^{1}t_m + {}^{2}t_m \quad (12)$$

or, in case the bed lengths and flow rates are equal in both dimensions ($^{1}t_m = {}^{2}t_m = t_m$):

$$^{2D}t_{w,spatial} = {}^{1}t_m + {}^{2}t_m = 2t_m \quad (13)$$

2.3. Calculation of the total dilution in $^{x}LC \times {}^{x}LC$

An important aspect in chromatographic analysis is the dilution of the analytes. Too much dilution will aggravate the detection problems that liquid chromatographers are all too often confronted with. Assuming that the concentration profiles of a sample spot (including the injection spot) follow a Gaussian distribution and that the law of mass conservation holds, one finds that the dilution factor (DF) can be expressed as

$$DF = \frac{h_{P,init}}{h_{P,fin}} = \frac{\sigma_{fin}}{\sigma_{init}} \quad (14)$$

where $h_{P,init}$ and $h_{P,fin}$ are the initial peak height and the peak height of a solute after development, respectively and σ_{init} and σ_{fin} the standard deviation of the initial sample spot and that after development, respectively.

The standard deviation after each development is a measure for the total spot broadening and can be expressed as [18]:

$$\sigma_{fin,1} = \sqrt{\sigma_i^2 + 2\gamma D_m t_m + xH_1} \quad (15)$$

$$\sigma_{fin,2} = \sqrt{\sigma_i^2 + 2\gamma D_m t_m + yH_2} \quad (16)$$

where $\sigma_{fin,1}$ and $\sigma_{fin,2}$ are the spot variances in length units after the two developments.

The total dilution (^{2D}DF) of the chromatographic process can subsequently be calculated from

$$^{2D}DF = {}^{1}DF \times {}^{2}DF \quad (17)$$

in which ^{1}DF and ^{2}DF are defined as the dilution experienced in the first and second dimension, respectively.

Implementing Eqs. (9) and (14)–(16) in Eq. (17) and again assuming equal bed characteristics in both directions yields:

$$^{2D}DF = 1 + \left(\frac{2\gamma D_m t_m + \frac{LH}{(k+1)}}{\sigma_i^2}\right) \quad (18)$$

3. Experimental

3.1. Parameters used

The use of Eqs. (2)–(18) allows connecting the total peak capacity to the total analysis time and the total dilution in an $^{x}LC \times {}^{x}LC$ system. Some parameters, such as the maximum pressure drop, particle size of the chromatographic bed and sample spot size given in Eqs. (2)–(18) can be defined by the user. Other parameters, such as van-Deemter coefficients (a, b, and c), viscosity, diffusion coefficient, bed tortuosity and resistance factor, and retention factors depend on the particular LC system. The typical values for the parameters used in Eqs. (2)–(18) are summarized in Table 1.

3.2. Computation of the Pareto front

Fig. 1 describes the process of calculating the chromatographic parameters using Eqs. (2)–(18). After the parameters have been defined as in Table 1, the first step is to fix the development time t_m. Note that, as we impose symmetrical conditions for the two (first- and second-dimension) developments, t_m is the same for both dimensions. At a fixed value of d_p, Eq. (2) is applied to obtain L (see Fig. 1). From the values of L and t_m, u_m can be calculated, and hence ν (Eq. (4)). Eq. (3) is then applied to calculate h, and (since d_p is known) the actual plate height, H. From there, the peak capacity of the system, the total analysis time and the total dilution are straightforwardly computed from Eqs. (10), (13) and (18), respectively. This process can be repeated for various combinations of values of d_p, t_m and σ_i (which constitute the experimental factors considered). All permutations are computed to find optimal conditions. In this study this was achieved using a simple Excel spreadsheet. The three variables had the following values (see Table 1). The development time varied from 5 s to 1800 s, the particle size varied between 4 and 12 μm, and the initial spot size varied from 0.5 to 4 mm. The development time was varied in steps of 5 s from 5 to 360 s and in steps of 30 s from 360 to 1800 s. The particle size was varied in steps of 0.1 μm from 4 to 8 μm and in steps of 1 μm from 8 to 12 μm. All combinations of factors resulted in 21,600 computations. The output

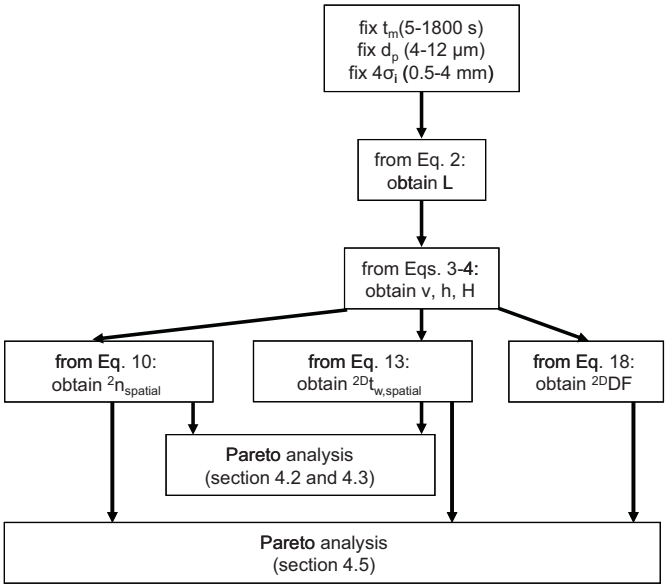

Fig. 1. Flowchart describing the process to calculate the different chromatographic parameters required to perform the two-objective (Sections 4.2 and 4.3) and three-objective (Section 4.5) Pareto analyses.

Table 1
Chromatographic parameters used in this study to calculate peak capacities, analysis times, and dilution factors in two-dimensional spatial LC. Where relevant, a reference is included.

Name	Value	Units	Equation	Reference
van-Deemter coefficient, a	0.5		(3)	[37]
van-Deemter coefficient, b	6		(3)	[37]
van-Deemter coefficient, c	0.4		(3)	[37]
Diffusion coefficient, D_m	10^{-9}	m^2/s	(4), (15), (16) and (18)	[23]
Maximum pressure drop, ΔP	0.5×10^7	Pa	(2)	[35]
Bed resistance factor, ϕ	1000		(2)	[23,37]
Bed thickness, d_b	0.1	mm		
Mobile-phase viscosity, η	10^{-3}	Pa s	(2)	[23]
Bed tortuosity, Y	0.75		(10), (11), (15), (16) and (18)	[18,28]
Particle size, d_p	4–12	μm	(2)	[37]
Resolution, R_s	1			
Development time in first and second dimension, t_m	5–1800	s	(2), (12), (13), (15), (16) and (18)	
Initial sample spot size, $4\sigma_i$,	0.5, 1, 2, 4	mm	(10), (15), (16) and (18)	[37]
Retention factor, k	1		(7)–(9) and (18)	

parameters (bed length, total peak capacity, total analysis time, total dilution, *etc.*) for each case were calculated using the procedure described above. A filtering step could follow, eliminating those cases that imply non-practical situations (for example, column beds exposed to excessive stress, see Section 4.2). Finally, after having defined the objectives of the optimization (peak capacity, time and, in some studies, dilution), the Pareto-optimization algorithm was applied to all cases. The Pareto-optimization principle has been described elsewhere [42] and will not be discussed here in detail. In short, this technique is based on inspecting only those experiments which are Pareto-optimal. This is the case when it is not possible to improve one of the objectives without worsening the other(s). In our framework, the set of Pareto-optimal cases (the so-called Pareto front) represents the limit of our possibilities in terms of obtaining the highest possible peak capacity in the shortest possible time and with the lowest possible dilution. One should note that the dimensionality of the Pareto front depends on the number of objectives. If two objectives are considered (*i.e.* maximize total peak capacity and minimize analysis time) the Pareto front is a (curved) line. In case of a three-objective optimization (*i.e.* maximize total peak capacity minimize analysis time and minimize dilution) the Pareto front is a surface in three-dimensional space.

To find the Pareto-optimal experiments from the Excel table mentioned above, a home-build Pareto-optimization routine was implemented in MATLAB 7.11 (The Mathworks, Natick, MA).

4. Results and discussion

4.1. Influence of initial spot size dimensions on total peak capacity

A study was carried out to verify the validity of Eq. (11), the approximated form of Eq. (10). To this aim, for each of the 21,600 combinations of factors mentioned above, the value of the two-dimensional peak capacity in ${}^x\text{LC} \times {}^x\text{LC}$ was calculated using Eq. (10) and Eq. (11). It was observed that, for the smallest spot size ($4\sigma_i = 0.5$ mm), the approximation contained in Eq. (11) is valid if one accepts deviations of up to 5%. Only in some cases (considering small particles and extremely short development times) the approximation is not valid. However, the number of cases in which the approximation implies a deviation of more than 5% dramatically increases for larger spot sizes. In these cases, the equation is not valid across the entire range of particle sizes under study. This is especially noteworthy for the largest spot size considered in our study ($4\sigma_i = 4$ mm). In this case, the approximated formula deviates more than 5% from the non-approximated expression in all cases (deviations of up to 86% were encountered).

This effect was discussed in [18]. In this paper, the maximum dimensions of the initial sample spot size were defined as

$$\sigma_i < \sqrt{0.1Ld_p} \tag{19}$$

which implies that small particles and a short chromatographic bed would require a small maximum spot size if Eq. (11) is applied. This confirms the observations discussed above. Since in our computations Eq. (11) is not applicable in a significant number of cases, we will make use of Eq. (10) through this paper. This allows us to consider larger initial spot sizes than indicated by Eq. (19).

4.2. Pareto analysis of two-dimensional systems in the column and spatial modes

Fig. 2 depicts an overlay of four Pareto fronts corresponding to different two-dimensional chromatographic systems. The solid line corresponds to the "standard" ${}^t\text{LC} \times {}^t\text{LC}$ system described in [23], in which the first- and second-dimension elution conditions are gradient and isocratic, respectively, at a ΔP of 40 MPa (HPLC × HPLC). The dashed line corresponds to an ultra-high performance system (with $\Delta P = 100$ MPa) in ${}^t\text{LC} \times {}^t\text{LC}$, in which both the first and second dimension elution are under gradient conditions (UHPLC × UHPLC).

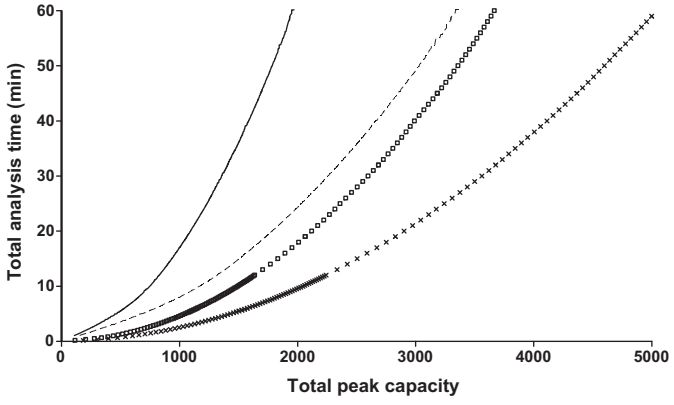

Fig. 2. Pareto fronts for the two-objective optimization of peak capacity and analysis time for two-dimensional liquid chromatography systems in the column and spatial modes. The solid and dashed lines correspond to a standard HPLC × HPLC system (gradient elution in first dimension, isocratic elution in the second dimension), and an ultra-high performance system (UHPLC × UHPLC, with gradient elution in both dimensions), respectively. Band-broadening effects are considered in both dimensions. Appropriate conditions and parameter values for both types of time-based chromatographic systems are given in [23]. The line represented by □ symbols illustrates the Pareto front for ${}^x\text{LC} \times {}^x\text{LC}$, using a sorbent bed of TLC quality. The line represented by the × symbol illustrates the Pareto front for ${}^x\text{LC} \times {}^x\text{LC}$, assuming a bed with HPLC-quality packing. Appropriate parameter values are listed in Table 1 and conditions are described in Section 3.

This curve is thought to represent the best that comprehensive two-dimensional column LC (*i.e.* ^{t}LC × ^{t}LC) can offer.

Both the solid and the dashed lines have been constructed while taking the band-broadening effects in both dimensions due to the use of modulation into account. For a more detailed explanation of the band broadening effects, choice of appropriate conditions, parameter values, and other relevant information concerning both types of ^{t}LC × ^{t}LC Ref. [23] should be consulted.

The curve formed by the □ symbols depicts the Pareto front for ^{x}LC × ^{x}LC, following Eqs. (2)–(18) and using the parameters listed in Table 1 and conditions described above (see Section 3). The curve formed by the × symbols illustrates the Pareto front for ^{x}LC × ^{x}LC in which the same packing efficiency is assumed as in conventional chromatographic columns. To obtain these results a Pareto analysis was performed using the reduced van-Deemter coefficients that were used in [23] (*i.e.* $a = 1.5$, $b = 1$, $c = 0.15$), instead of $a = 0.5$, $b = 6$ and $c = 0.4$, while leaving the other parameters and conditions the same.

The solid and dashed lines represent the limit of our possibilities with packed columns and conventional HPLC systems and ultra-high-performance LC instruments, respectively, in ^{t}LC × ^{t}LC. The results depicted in Fig. 2 for the conventional (HPLC) case concern a system in which gradient elution is applied in the first dimension and isocratic elution in the second (gradient × isocratic). This is the standard situation in our laboratory, but a good deal of work has also been published applying gradient conditions in both dimensions (examples see Refs. [43–47]). In the latter case higher peak capacities are generally obtained, but the total analysis time would be higher due to the re-equilibration time needed if a single second-dimension column and solvent-delivery system are used. Pareto analysis for conventional gradient × gradient HPLC has been discussed in [23].

Fig. 2 shows a clear advantage of two-dimensional spatial chromatography over the time-based (column) chromatography. To obtain the same total peak capacity the analysis time can be significantly shortened. Using an existing OPTLC apparatus with TLC-quality beds (square boxes in Fig. 2) one can observe that the spatial mode outperforms HPLC × HPLC (solid line) and even UHPLC × UHPLC (dashed line). For example, to achieve a peak capacity of 2000, an analysis time of 60 min, 24 min, and 18 min would be required for HPLC × HPLC, UHPLC × UHPLC, and ^{x}LC × ^{x}LC, respectively. This would imply a reduction in analysis time of 70% in comparison with HPLC × HPLC and 25% in comparison with UHPLC × UHPLC.

If we learn to pack thin beds as efficiently as packed columns, only 10 min would be required to achieve a peak capacity of 2000. This would imply a gain in analysis time of 83% with respect to HPLC × HPLC and 58% when compared with UHPLC × UHPLC.

The fundamental reason for these great gains in analysis time when using the spatial mode is the simultaneous separation of the entire sample in the second dimension. Also, the time restrictions for the second dimension become largely irrelevant, because this separation has to be performed only once. In contrast, in time-based separations the analysis time for the second dimension should be the same as the modulation time. A long modulation time yields a major gain in the second-dimension peak capacity (due to longer chromatograms). However, this is accompanied with a loss in peak capacity in both dimensions (due to "undersampling" in the first dimension and increased injection band broadening in the second dimension). The balance between the positive and negative effects has been discussed by Horie et al. [21] and by Vivó-Truyols et al. [23].

In spatial chromatography all second-dimension elutions are performed simultaneously. Hence, there is no need to strike a compromise. Furthermore, since no modulation (valve) is needed for ^{x}LC × ^{x}LC, the above-mentioned additional band-broadening (due to "undersampling" and second-dimension injection volume) is avoided. However, it follows from Eqs. (10) that large peak capacities in ^{x}LC × ^{x}LC require large two-dimensional separation beds. Even in combination with a moderate pressure drop of 5 MPa (50 bar or 730 psi), this would require extremely large forces on the spatial chromatographic device. This will be addressed in the next section.

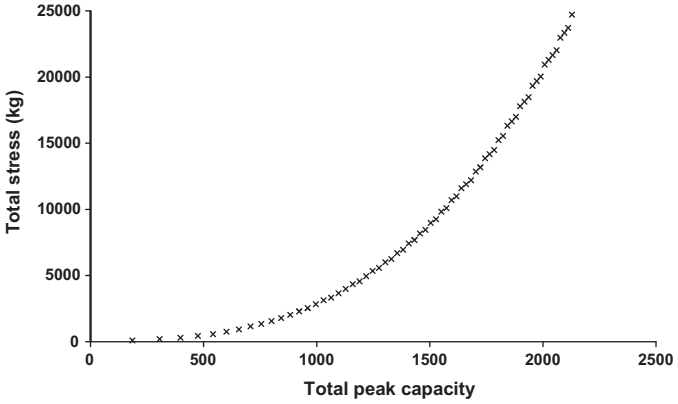

Fig. 3. Pareto front for ^{x}LC × ^{x}LC with HPLC packing efficiency illustrating the achievable peak capacity as a function of the total stress required using parameters listed in Table 1 and conditions as described in Section 3.

4.3. Constrained optimization

Fig. 3 indicates the total peak capacity in well-packed ^{x}LC × ^{x}LC as a function of the total stress required, using $a = 1.5$, $b = 1$ and $c = 0.15$ in Eq. (3). Interestingly, one observes that the curve is relatively flat for values of peak capacity up to around 1000. However, at higher values for the total peak capacity the total required force increases strongly. As a consequence, a minor gain in peak capacity requires a substantial increase in the total force applied on the chromatographic device. Much greater forces are required in the region of high n_c values. A stress of 20,000 kg is needed to obtain a peak capacity of around 2000; an additional 100 in peak capacity would require an extra 3500 kg of stress. Such extremely high stresses may be difficult to deal with in practice. They have not been considered in the present study to avoid creating unrealistic expectations.

Consequently, the Pareto front for well-packed beds in ^{x}LC × ^{x}LC shown in Fig. 2 was modified by imposing a restriction on the maximum permissible stress. If a maximum stress of 2500 kg is allowed, then the maximum bed length corresponding to a pressure drop of 5, 4, 3, 2, 1.5, and 1 MPa is 100 mm, 111.8 mm, 129 mm, 158.1 mm, 182.6 mm, and 223.6 mm, respectively. Considering the maximum pressure drop as a variable (varying between 5 and 1 MPa) and applying the same procedure as in Section 3.2, a new Pareto front is obtained.

Fig. 4 illustrates an enlarged area of Fig. 2. The Pareto front constituting of the × symbols corresponds to ^{x}LC × ^{x}LC using a bed of HPLC quality, without any restrictions applied. The points denoted with the ● symbol include a limit on the maximum stress as mentioned above. For peak capacities below 1100 the two Pareto fronts overlap. At peak capacities above 1100, the stress restriction causes the Pareto front to rise steeply. This can be explained from the Pareto optimal results for the bed length, particle size, and pressure drop for the restricted variant of ^{x}LC × ^{x}LC, shown in Fig. 5A–C, respectively.

Fig. 5C indicates that up to peak capacities of around 1100, the Pareto-optimal pressure drop corresponds to the maximum allowable system pressure in ^{x}LC × ^{x}LC, which explains the overlap with the unrestricted Pareto front. However, at higher values for the peak

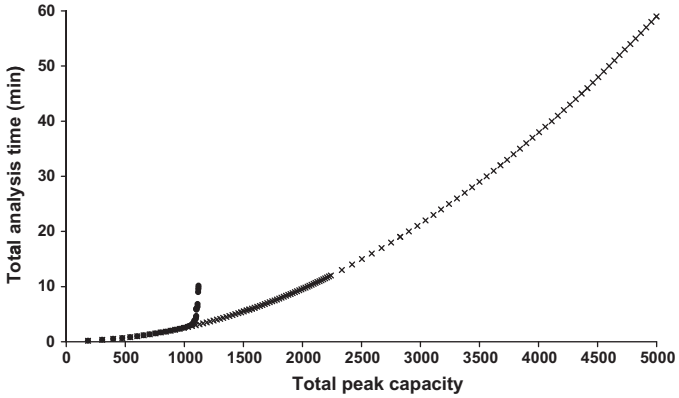

Fig. 4. Pareto fronts representing ^{x}LC × ^{x}LC, assuming a sorbent bed with HPLC packing quality. The line represented by the × symbol corresponds to an optimization without stress restrictions; the line formed by the ● symbols refers to the limit of our possibilities imposing a maximum stress of 2500 kg. For parameter values see Table 1 and for conditions see Section 3.

capacity, the stress limit can only be met by increasing the particle size and the bed length and reducing the pressure drop. Eq. (2) and Eq. (10) indicate that at lower pressures a higher peak capacity can be achieved by increasing the bed length L in combination with an increase in particle size d_p. This is clearly observed in Fig. 5A and B. The situation is fully analogous to what is encountered in conventional one-dimensional column LC.

However, as can be observed from Fig. 5B the optimal particle size decreases at a certain point before it increases again. This decrease might be explained by the fact that in the region where this phenomena occurs the maximum allowable bed length (100 mm, corresponding at 5 MPa pressure) has been reached. From the Darcy equation (Eq. (2)) the bed length L can now be seen as a fixed parameter. A further increase in development time t_m in order to obtain higher peak capacities will result in a decrease in particle size d_p since all other parameters in this equation are now fixed. In the region where lower pressures are found to be Pareto optimal (see Fig. 5C), longer beds packed with larger particles may be used.

If one now considers the bed to have maximum dimensions of 100 × 100 mm (equivalent to common stainless-steel MALDI plates), then a maximum peak capacity of 780 in 2.7 min can be obtained under practical ^{x}LC × ^{x}LC conditions (data not shown). In case of well-packed packed beds, one may ultimately obtain a peak capacity of around 1020 in 2.7 min in the ^{x}LC × ^{x}LC mode (see Fig. 5A and D). This corresponds to a peak-production rate of about 6.3 peaks/s, which is, for example, 12 times higher than the value for the impressive on-line ^{t}LC × ^{t}LC separation of plant metabolites reported by Stoll et al. [25].

4.4. Expanding the limits of ^{x}LC × ^{x}LC: hypothetical use of higher pressures and smaller particles

As explained above, investing in the development of two-dimensional OPTLC devices is promising, since they can generate higher peak-production rates than the best time-based two-dimensional (UHPLC × UHPLC) systems on the market. In order to further increase the peak-production rates, while avoiding the use of very large beds, one may consider the use of elevated pressures. It follows from the previous paragraph that an increase in pressure does not only result in shorter bed lengths, but also in smaller particles.

To demonstrate the potential increase in peak-production rates, a Pareto analysis applying extreme conditions (40 MPa, 1–12 μm particles) was performed for ^{x}LC × ^{x}LC, using TLC-quality beds (data not shown). For a 100 mm × 100 mm bed, a maximum peak capacity

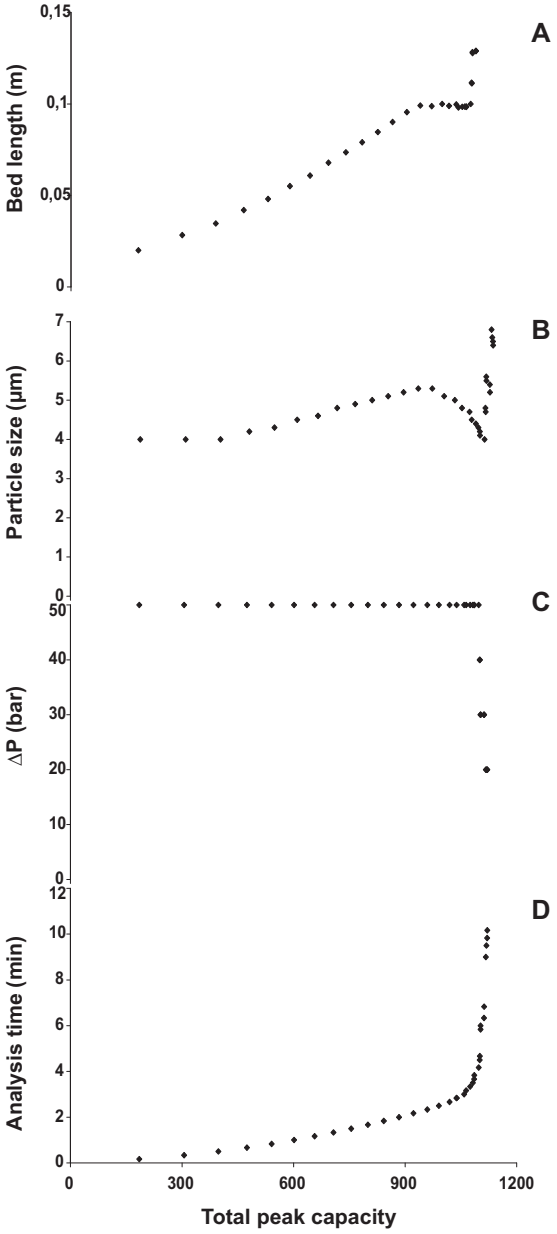

Fig. 5. Pareto-optimal results for optimization of peak capacity and analysis time in ^{x}LC × ^{x}LC assuming a sorbent bed of HPLC packing quality, imposing a stress limitation of 2500 kg, and using parameters from Table 1 and conditions as described Section 3. In parts A–D, the x-axis corresponds to the total peak capacity (same axis for all four plots). y-axis: (A) optimal bed lengths in both dimensions; (B) optimal particle sizes in both dimensions; (C) optimal pressure drop in both dimensions; (D) total analysis time.

of 1460 may ultimately be obtained in an analysis time of 1.3 min. This would imply a 3- to 4-fold increase in peak-production rate in comparison with the 5 MPa conditions. However, to counterbalance for the pressure drop across the 100 mm × 100 mm separation bed, a compensating force of 20,000 kg would need to be applied.

One should be aware that, apart from the high stresses required, the use of high pressures in liquid chromatography may influence the different experimental parameters used, as was investigated in detail in [48]. It was shown that the pressure dependence of, for example, the mobile phase density and viscosity, the diffusion coefficients, the particle size, the retention factors, the efficiency parameters, *etc.* is negligible, as long as pressures do not exceed a few tens of MPa. As a result, the Pareto-optimal results obtained in Sections 4.1–4.3 through the use of Eqs. (2)–(18) and using a 5-MPa

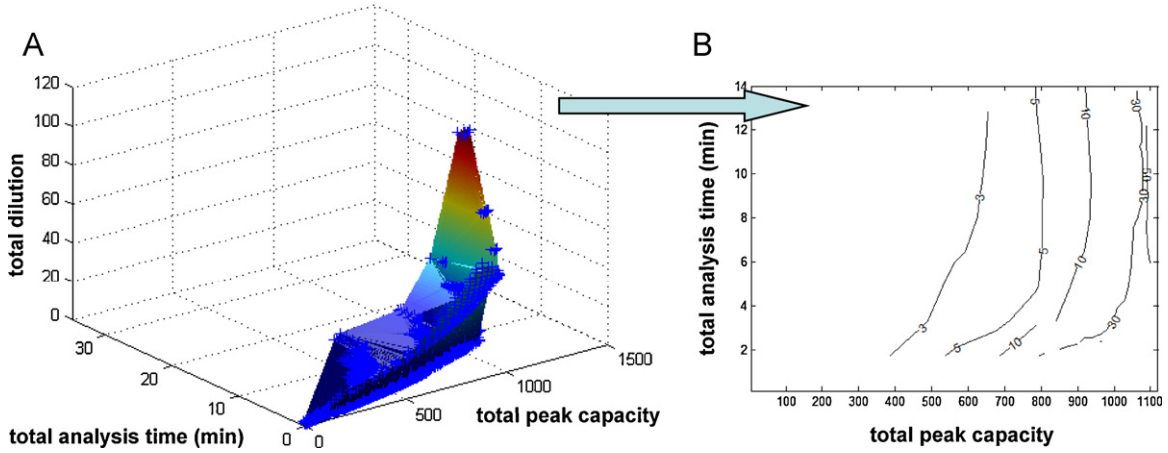

Fig. 6. (A) Pareto-optimal surface obtained from a three-objective optimization (maximal total peak capacity, minimal total analysis time and minimal total dilution) for ^{x}LC × ^{x}LC with a sorbent bed of HPLC quality and applying a stress limitation of 2500 kg. For parameter values see Table 1 and for conditions see Section 3. Symbols represent actual Pareto experiments. The surface is defined by linear interpolation between these points. Part (B) represents the surface depicted in (A) through constant-dilution lines in a peak capacity *vs.* analysis time plot.

pressure limit in ^{x}LC × ^{x}LC may be seen as valid. However, at higher pressures (*e.g.* 40 MPa or even higher) deviations become more significant and the validity of Eqs. (2)–(18) may be questioned.

A possible way to circumvent the use of higher system pressures may be to work at elevated temperatures to decrease the mobile-phase viscosity, as has been amply demonstrated in ^{t}LC × ^{t}LC [47,49–51]. Higher temperatures would enhance the performance of ^{x}LC × ^{x}LC even when short bed lengths are used and relatively low pressures.

Another way to achieve high-resolution ^{x}LC × ^{x}LC separations may be to combine electrically driven and pressure-driven flows [29,52]. In the latter study the mobile phase was transported

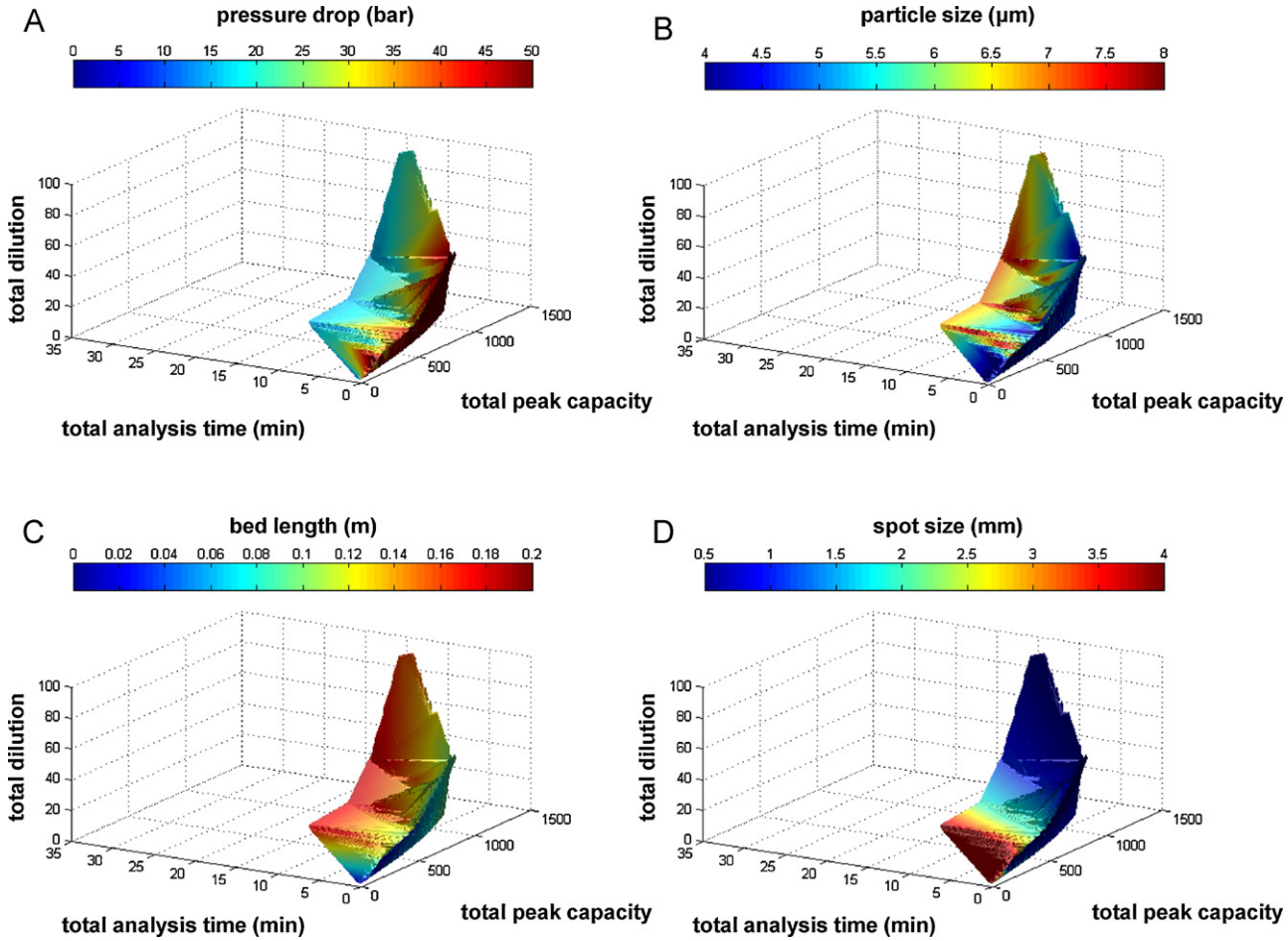

Fig. 7. Pareto-optimal results for pressure drop (A), particle size (B), bed length (C), and initial spot size (D) along the Pareto-optimal surface of Fig. 6A. Parameter values are indicated through a color coding (top bars).

by an electro-osmotic flow, while the sorbent layer was pressurized to allow efficient heat dissipation from the layer through an electrically insulating and thermally conducting sheet of ceramic aluminium-nitride. Only one-dimensional separations were demonstrated. However, such separation systems are beyond the scope of the present study and they will not be considered further.

4.5. Effect of dilution in $^{x}LC \times {}^{x}LC$: trade-off between analysis time, peak capacity, and dilution

So far, we have considered only the minimization of the analysis time and the maximization of the peak capacity of two-dimensional systems. From a practical point of view, however, the experimenter would like to find those optimal conditions that maintain other relevant parameters within a reasonable range. One such parameter is the dilution experienced by the sample. A simple way to keep dilution under control is to select this parameter as an objective in a Pareto optimization.

The results of a three-objective Pareto optimization imposing a restriction of 2500 kg on the total stress (see Section 4.3) for $^{x}LC \times {}^{x}LC$ using a well-packed bed (ΔP ranging from 1 to 5 MPa, d_p from 4 to 12 μm) are shown in Fig. 6. The Pareto front resulting from a three-objective optimization, representing the limit of our possibilities, is no longer a line but a surface. A simplified and more quantitative representation of the surface is given by the contour lines (at equal dilution) in Fig. 6B.

Each constant-dilution line represents the most favorable trade-off between analysis time and peak capacity for a fixed value of the total dilution. One should note that the constant-dilution lines are calculated by interpolation. Therefore, the surface is poorly defined.

From Fig. 6A it can be observed that the surface is quite steep around the best trade-off between time and peak capacity. This indicates that a large decrease in dilution only results in a minor loss in peak capacity and/or a minor increase in time. This is clearly observed in Fig. 6B. Decreasing the dilution from, for example, 50 to 30 will not significantly decrease the total peak capacity and increase the analysis time. However, if we want the dilution to be decreased even more, for example to a value of 10 or 5, a greater loss in peak capacity and/or speed will have to be accepted.

It is instructive to inspect the optimal values of the parameters along the Pareto surface. Fig. 7 illustrates the results of this analysis. The values of the respective parameters are assigned a color, which is then projected on the surface of Fig. 6A. Fig. 7A–D reveal that neither the pressure, nor the particle size nor the bed length have a great influence on the high dilution rates (the color of the surface does not change when descending along the steepest face of the surface), where dilution varies greatly, without affecting the trade-off between peak capacity and analysis time. In contrast, as can be observed in Fig. 7D, by changing the initial spot size from 0.5 to 1 mm, a significant decrease in the dilution factor is obtained, at almost no cost in peak capacity and/or time. This is achieved while leaving the other parameters almost unchanged. For example, by increasing the spot size from 0.5 to 1 mm the dilution factor may be decreased from 108 to 28, while the peak capacity only decreases from 1117 to 1072, leaving the other parameters (analysis time, pressure, particle size, and bed length) unaffected. However, by increasing the spot size even more (*e.g.* to 4 mm), a much greater negative impact on the trade-off between peak capacity and analysis time is observed (see Fig. 7D).

In summary, under reasonable (stress) conditions high peak capacities, short analysis times, and low dilution factors can be obtained by using high pressures, short beds, and small particles and by applying relatively large sample spots on the chromatographic bed.

5. Conclusions

On-line, real-time, comprehensive two-dimensional time-based (column) liquid chromatography is frequently used to obtain high peak capacities within a reasonable time. However, the possibilities to achieve attractive trade-offs between peak capacity and analysis time are limited. In this study we used a Pareto-optimality approach to evaluate the potential of spatial two-dimensional chromatography, *i.e.* a system in which the separations are achieved using a porous medium to separate a sample in two (or ultimately three) dimensions and the sample is separated two (or three) times in perpendicular directions. Analytes are separated according to their specific location in the plane, rather than their time of elution, as in the case of column-based liquid chromatography. Spatial chromatography was found to outperform time-based chromatography in terms of (minimum) time and (maximum) peak capacity.

However, due to severe stress requirements, extremely high peak capacities may be difficult to achieve. In the immediate future this type of liquid chromatography may be most attractive for very fast analysis of relatively complex samples, rather than for extremely efficient separations. For example, by restricting the stress to 2500 kg, a peak capacity of 780 may be achieved in only 2.7 min when using a 100 mm × 100 mm sorbent bed. If sorbent beds could be packed with HPLC packing quality, the peak capacity would further increase to around 1020.

Dilution factors may become excessive if very small injection volumes (spot sizes) are applied. We performed a Pareto-optimization study using three objectives (minimal analysis time/maximal peak capacity/minimal dilution). In this later optimization the injection spot size proved to be one of the key parameters. Increasing the injection spot size from 0.5 mm to 1 mm did not increase the analysis time, nor significantly decrease the peak capacity, but it reduced the dilution factor from 108 to 28.

Even higher performances may ultimately be achieved if three-dimensional spatial chromatographic separations can be carried out. This would imply using a three-dimensional separation body, in which the analytes would be separated sequentially along the *x*-, *y*-, and *z*-axis. Each separated compound will then be characterized by a combination of its *x*, *y*, and *z*-coordinates in the separation body.

Acknowledgment

This work was financially supported by NWO, the Netherlands Organization for Scientific Research (project C.2322.0129).

References

[1] J.C. Giddings, Anal. Chem. 39 (1967) 1027.
[2] J.M. Davis, J.C. Giddings, Anal. Chem. 55 (1983) 418.
[3] T. Wehr, LC–GC North Am. (2002) 954.
[4] S. Eeltink, S. Dolman, F. Detobel, R. Swart, M. Ursem, P.J. Schoenmakers, J. Chromatogr. A 1217 (2010) 6610.
[5] M. Gilar, A.E. Daly, M. Kele, U.D. Neue, J.C. Gebler, J. Chromatogr. A 1061 (2004) 183.
[6] G. Guiochon, J. Chromatogr. A 1126 (2006) 6.
[7] Q. Luo, Y. Shen, K.K. Hixson, R. Zhao, F. Yang, R.J. Moore, H.M. Mottaz, R.D. Smith, Anal. Chem. 77 (2005) 5028.
[8] J.E. MacNair, K.D. Patel, J.W. Jorgenson, Anal. Chem. 71 (1999) 700.
[9] N. Marchetti, A. Cavazzini, F. Gritti, G. Guiochon, J. Chromatogr. A 1163 (2007) 203.
[10] N. Marchetti, J.N. Fairchild, G. Guiochon, Anal. Chem. 80 (2008) 2756.
[11] K. Miyamoto, T. Hara, H. Kobayashi, H. Morisaka, D. Tokuda, K. Horie, K. Koduki, S. Makino, O. Nuñez, C. Yang, T. Kawabe, T. Ikegami, H. Takubo, Y. Ishihama, N. Tanaka, Anal. Chem. 80 (2008) 8741.
[12] U.D. Neue, J. Chromatogr. A 1184 (2008) 107.
[13] P. Sandra, G. Vanhoenacker, J. Sep. Sci. 30 (2007) 241.
[14] Y. Shen, R. Zhang, R.J. Moore, J. Kim, T.O. Metz, K.K. Hixson, R. Zhao, E.A. Livesay, H.R. Udseth, R.D. Smith, Anal. Chem. 77 (2005) 3090.
[15] X. Wang, D.R. Stoll, A.P. Schellinger, P.W. Carr, Anal. Chem. 78 (2006) 3406.
[16] H. Poppe, J. Chromatogr. A 778 (1997) 3.

[17] J.C. Giddings, Anal. Chem. 56 (1984) 1258A.
[18] G. Guiochon, L.A. Beaver, M.F. Gonnord, A.M. Siouffi, M. Zakaria, J. Chromatogr. 255 (1983) 415.
[19] F. Bedani, W.T. Kok, H.-G. Janssen, J. Chromatogr. A 1133 (2006) 126.
[20] L.M. Blumberg, J. Sep. Sci. 31 (2008) 3358.
[21] K. Horie, H. Kimura, T. Ikegami, A. Iwatsuka, N. Saad, O. Fiehn, N. Tanaka, Anal. Chem. 79 (2007) 3764.
[22] R.E. Murphy, M.R. Schure, J.P. Foley, Anal. Chem. 70 (1998) 1585.
[23] G. Vivó-Truyols, S. van der Wal, P.J. Schoenmakers, Anal. Chem. 82 (2010) 8525.
[24] J.N. Fairchild, K. Horváth, G. Guiochon, J. Chromatogr. A 1216 (2009) 1363.
[25] D.R. Stoll, X. Wang, P.W. Carr, Anal. Chem. 80 (2007) 268.
[26] S. Eeltink, S. Dolman, R. Swart, M. Ursem, P.J. Schoenmakers, J. Chromatogr. A 1216 (2009) 7368.
[27] G. Guiochon, M. Gonnord, M. Zakaria, L. Beaver, A. Siouffi, Chromatographia 17 (1983) 121.
[28] G. Guiochon, N. Marchetti, K. Mriziq, R.A. Shalliker, J. Chromatogr. A 1189 (2008) 109.
[29] D.J.D. Vanhoutte, S. Eeltink, W.T. Kok, P.J. Schoenmakers, Anal. Chim. Acta 701 (2011) 92.
[30] J. Klose, U. Kobalz, Electrophoresis 16 (1995) 1034.
[31] A.G. Chambers, J.S. Mellors, W.H. Henley, J.M. Ramsey, Anal. Chem. 83 (2011) 842.
[32] A.J. Link, Trends Biotechnol. 20 (2002) s8.
[33] T. Rabilloud, M. Chevallet, S. Luche, C. Lelong, J. Proteomics 73 (2010) 2064.
[34] E. Tyihák, E. Mincsovics, H. Kalász, J. Chromatogr. 174 (1979) 75.
[35] S. Nyiredy, Trends Anal. Chem. 20 (2001) 91.
[36] E. Tyihák, E. Mincsovics, H. Kalász, J. Chromatogr. 191 (1980) 293.
[37] S.K. Poole, C.F. Poole, J. Chromatogr. A 1218 (2011) 2648.
[38] L.A. Beaver, G. Guiochon, US Patent 4,469,601 (1984).
[39] J.A. Abia, J. Putnam, K. Mriziq, G.A. Guiochon, J. Chromatogr. A 1217 (2010) 1695.
[40] K.S. Mriziq, G. Guiochon, J. Chromatogr. A 1187 (2008) 180.
[41] C. Cramers, J. Rijks, C. Schutjes, Chromatographia 14 (1981) 439.
[42] D.L. Massart, B.G.M. Vandeginste, L.M.C. Buydens, S. de Jong, P.J. Lewi, J. Smeyers-Verbeke, Handbook of Chemometrics and Qualimetrics: Part A, Elsevier, Amsterdam, The Netherlands, 1997, p. 790.
[43] P. Cesla, T. Hájek, P. Jandera, J. Chromatogr. A 1216 (2009) 3443.
[44] P. Dugo, V. Skeříková, T. Kumm, A. Trozzi, P. Jandera, L. Mondello, Anal. Chem. 78 (2006) 7743.
[45] T. Ikegami, T. Hara, H. Kimura, H. Kobayashi, K. Hosoya, K. Cabrera, N. Tanaka, J. Chromatogr. A 1106 (2006) 112.
[46] H. Kimura, T. Tanigawa, H. Morisaka, T. Ikegami, K. Hosoya, N. Ishizuka, H. Minakuchi, K. Nakanishi, M. Ueda, K. Cabrera, N. Tanaka, J. Sep. Sci. 27 (2004) 897.
[47] D.R. Stoll, J.D. Cohen, P.W. Carr, J. Chromatogr. A 1122 (2006) 123.
[48] M. Martin, G. Guiochon, J. Chromatogr. A 1090 (2005) 16.
[49] A. Ginzburg, T. Macko, V. Dolle, R. Brüll, J. Chromatogr. A 1217 (2010) 6867.
[50] D.R. Stoll, X. Li, X. Wang, P.W. Carr, S.E.G. Porter, S.C. Rutan, J. Chromatogr. A 1168 (2007) 3.
[51] Y. Wei, T. Lan, T. Tang, L. Zhang, F. Wang, T. Li, Y. Du, W. Zhang, J. Chromatogr. A 1216 (2009) 7466.
[52] D. Nurok, J.M. Koers, A.L. Novotny, M.A. Carmichael, J.J. Kosiba, R.E. Santini, G.L. Hawkins, R.W. Replogle, Anal. Chem. 76 (2004) 1690.